Observation of a Very Massive Galaxy Cluster at $z = 0.76$ in the SRG/eROSITA All-Sky Survey

R. A. Burenin[1*], I. F. Bikmaev[2,3], M. R. Gilfanov[1,4], A. A. Grokhovskaya[5], S. N. Dodonov[5], M. V. Eselevich[6], I. A. Zaznobin[1], E. N. Irtuganov[2,3], N. S. Lyskova[1], P. S. Medvedev[1], A. V. Meshcheryakov[1], A. V. Moiseev[1,5], S. Yu. Sazonov[1], A. A. Starobinsky[7], R. A. Sunyaev[1,4], R. I. Uklein[5], I. I. Khabibullin[1,4], I. M. Khamitov[2,8], and E. M. Churazov[1,4]

[1]*Space Research Institute, Russian Academy of Sciences, Moscow, 117997 Russia*

[2]*Kazan Federal University, Kazan, 420000 Russia*

[3]*Academy of Sciences of Tatarstan, Kazan, Russia*

[4]*Max Planck Institut für Astrophysik, Karl-Schwarzschild-Str. 1, Postfach 1317, D-85741 Garching, Germany*

[5]*Special Astrophysical Observatory, Russian Academy of Sciences, Nizhnii Arkhyz, Karachai-Cherkessian Republic, 369167 Russia*

[6]*Institute of Solar−Terrestrial Physics, Russian Academy of Sciences, Siberian Branch, Irkutsk, 664033 Russia*

[7]*Landau Institute for Theoretical Physics, Russian Academy of Sciences, Chernogolovka, Russia*

[8]*TÜBITAK National Observatory, Antalya, Turkey*

Abstract—The results of multiwavelength observations of the very massive galaxy cluster SRGe CL2305.2−2248 detected in X-rays during the first SRG/eROSITA all-sky survey are discussed. This galaxy cluster has also been detected previously in the millimeter band in the South Pole Telescope (SPT-CL J2305−2248) and Atacama Cosmology Telescope (ACT-CL J2305.1−2248) surveys through the observation of the Sunyaev−Zeldovich effect. The spectroscopic redshift has been measured at the 6-m BTA telescope, $z = 0.7573$. In addition, deep photometric measurements of galaxies have been performed at the Russian−Turkish 1.5-m telescope (RTT-150). The mass of the cluster is estimated from the eROSITA data to be $M_{500} = (9.0 \pm 2.5) \times 10^{14}\ M_{\odot}$. We show that this cluster is among several tens of the most massive clusters in the observable Universe and among only a few most massive galaxy clusters at $z > 0.6$.

1. INTRODUCTION

It is expected that $\sim$100 000 galaxy clusters, including all clusters with masses above $M_{500} \approx 3 \times 10^{14}\ M_{\odot}$ in the observable Universe, will be detected in the all-sky X-ray survey with the eROSITA telescope onboard the Spectrum−Roentgen−Gamma (SRG) observatory (Sunyaev et al. 2021; Predehl et al. 2021). Clearly, this sample will be of enormous interest for various cosmological studies. For example, these data will allow one to obtain new constraints on the parameters of the cosmological model and the dependence $\sigma_8(z)$ using the measurements of galaxy cluster mass functions (see, e.g., Vikhlinin et al. 2009b; Ade et al. 2014, 2016b), which, in turn,

will give an independent method to determine the redshift dependence of the Hubble parameter $H(z)$ (see, e.g., L'Huillier et al. 2020).

The all-sky survey was started in December 2019, after the successful launch of the SRG space observatory in July of the same year. At present, two complete all-sky surveys have been carried out with the SRG telescopes. The available eROSITA data allow an all-sky survey whose depth is greater than the depth of the ROSAT X-ray survey by almost an order of magnitude to be obtained. This makes it possible detect all of the most massive galaxy clusters in the observable Universe, with masses above $M_{500} \approx 6 \times 10^{14}\ M_{\odot}$ located at redshifts up to $z \approx 1$, already now.

*E-mail: rodion@hea.iki.rssi.ru

Such galaxy clusters are also observed in the Planck all-sky survey (Ade et al. 2016a, PSZ2). However, it turns out that not all of the very massive clusters at high redshifts were included in the PSZ2 catalog. Some of these clusters were later identified in the optical band among the Sunyaev−Zeldovich (SZ) sources of the PSZ2 catalog (see, e.g., Burenin et al. 2018; Zaznobin et al. 2019). In addition, some of these galaxy clusters were not included in the PSZ2 catalog.

In this paper we discuss the observation of the very massive galaxy cluster SRGe CL2305.2−2248 detected in the SRG/eROSITA all-sky survey. Using optical observations at the Russian-Turkish 1.5-m Telescope (RTT-150) and the 6-m BTA telescope of the Special Astrophysical Observatory of the Russian Academy of Sciences (SAO RAS), we obtained deep photometric data for the field of this cluster and a measurement of its spectroscopic redshift. Previously, this cluster has also been observed in the South Pole Telescope (Bleem et al. 2020) and Atacama Cosmology Telescope (Hilton et al. 2021) surveys in the millimeter band. The cluster mass estimates obtained by various methods agree well between themselves. This cluster is shown to be is one of the few most massive clusters in the observable Universe at a redshifts $z > 0.6$.

2. OBSERVATIONS IN THE SRG/eROSITA SURVEY

As of the beginning of June 2021, the field of the galaxy cluster SRGe CL2305.2−2248 was observed in the SRG/eROSITA all-sky survey three times— in June and December 2020 and in May 2021. The total exposure time corrected for vignetting was about 250 s. The eROSITA data were processed with the eSASS[1] software using preflight calibration data. An X-ray image of the SRGe CL2305.2−2248 field in the 0.5−2 keV energy band is shown in Fig. 2 on the upper left panel. In total, about 140 photons were recorded from this source during the first year of the SRG/eROSITA survey. The search for sources in the all-sky survey was carried out using the wavelet decomposition of X-ray images (Vikhlinin et al. 1998), and then various characteristics of sources were calculated by the maximum likelihood method with the ermldet software from the eSASS package. In this field, in the all-sky survey a previously unknown extended X-ray source with the coordinates of its center $\alpha = 23^{\mathrm{h}}05^{\mathrm{m}}11\overset{\mathrm{s}}{.}6$ and $\delta = -22^{\mathrm{d}}48^{\mathrm{m}}54^{\mathrm{s}}$ was detected. Assuming that the radial surface brightness profile of the extended source is described by the β-model, $I = I_0(1 + r^2/r_c^2)^{-3\beta+0.5}$ (Cavaliere and Fusco-Femiano

1976) with $\beta = 2/3$, the significance of the source's extent corresponds to $\delta\chi^2 = 30.66$, i.e., it is high, the radius of the β-model is $r_c = 20\overset{\prime\prime}{.}1$. The X-ray flux from the source in the 0.5−2 keV energy band calculated with ermldet and corrected for interstellar absorption in the Galaxy with a column density $N_{\mathrm{H}} = 2.2 \times 10^{20}$ cm^{-2} is $6.62 \pm 0.61 \times 10^{-13}$ erg s^{-1} cm^{-2}.

Note that the central part of the extended X-ray source looks perturbed, which may be the result of an outflow of hot gas from the active nucleus of one of the central galaxies in the cluster. On the other hand, this may also be a consequence of large-scale gas motions.

Figure 1 shows the spectrum of the extended X-ray source from the SRG/eROSITA data. The spectrum was extracted from a circle of radius $5'$ centered on the cluster. The detector background induced by charged particles was removed using calibration observations, in which the detector was covered by a filter opaque to X-ray photons. The X-ray sky background toward the cluster was estimated in a $5'-50'$ annulus around the cluster and was subtracted from the spectrum. The statistical significance of the data does not allow an upper limit on the gas temperature to be placed, but excludes a temperature below 3 keV at the 2 σ level. Figure 1 shows the model spectrum of an optically thin plasma with a temperature of 11 keV, which roughly corresponds to the temperature−luminosity relation for a given redshift (see below).

3. OPTICAL AND INFRARED OBSERVATIONS

3.1. Direct Imaging and Photometry

A massive galaxy cluster was detected in the field of the extended X-ray source with an automated procedure for the identification of galaxy clusters in the optical and infrared ranges using data from the Pan-STARRS (Chambers et al. 2016) and WISE (Wright et al. 2010) surveys, which is based on the search for the red sequence of galaxies. For this purpose, we used the WISE coadds obtained from the data in the full WISE operation time (Meisner et al. 2017), the NeoWISE-R6 versions, accessible on the Internet.[2] We used the forced photometry based on these WISE data for all objects from the Pan-STARSS survey obtained with a complete model of the point spread function (PSF), which correctly takes into account not only its wings on large angular scales, but also its asymmetry relative to the center (Burenin et al. 2021). We searched for the red sequence with an automated procedure similar to that used in Burenin (2017). The

---

[1] https://erosita.mpe.mpg.de/edr/DataAnalysis/.

[2] http://unwise.me/.
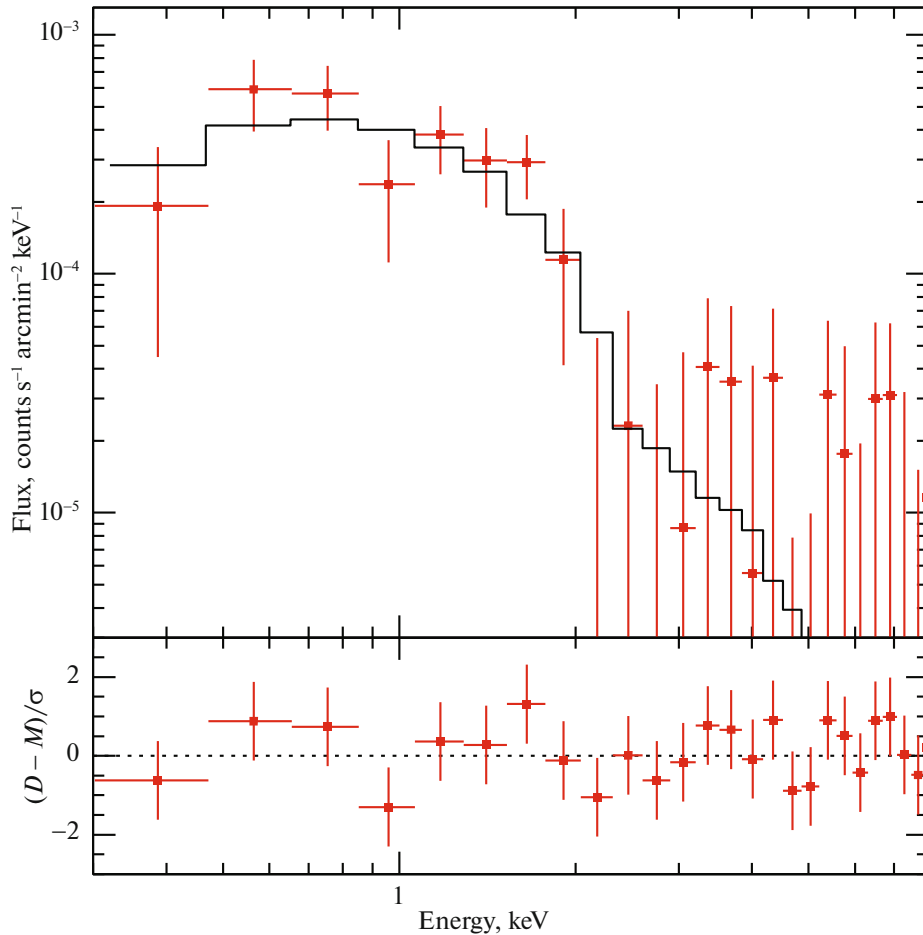
Fig. 1. Spectrum of the extended X-ray source SRGe CL2305.2−2248 from the SRG/eROSITA data. The solid curve indicates the model spectrum—the radiation of an optically thin plasma with a temperature $kT = 11$ keV. The statistical significance of the data allows to a temperature below 3 keV to be excluded at the 2σ level. The flux was normalized to 1 arcmin^2 and one of the seven eROSITA modules.

photometric redshift estimate from the red-sequence colors is $z_{phot} = 0.70 \pm 0.04$.

Deep direct images of the field of the galaxy cluster SRGe CL2305.2−2248 were obtained at the Russian−Turkish 1.5-m Telescope (RTT-150) in the quota of time of the Kazan Federal University from August 23 to 26, 2020, in the SDSS g, r, i, and z filters. The total exposure times were 13 200, 13 800, 8400, and 8400 s, respectively. The seeing was about 1″5. The total exposure time in each filter was divided into 600-s exposure times between which the telescope pointing axis was shifted by 10″−20″ in an arbitrary direction. The direct images were reduced in a standard way, using the IRAF package and our own software, with the application of a standard set of calibrations. A pseudo-color image of this field in the i, r, g (RGB) filters is shown in Fig. 2 on the upper right panel. The red galaxies at the image center are cluster members.

Photometric calibration of the images was ob-

tained using the observations of photometric standards for Smith et al. (2002) and by a comparison with the Pan-STARSS photometric measurements (Chambers et al. 2016). Figure 3 shows the color−magnitude diagram for galaxies in the cluster field within 3′3 of the X-ray center of the cluster. To construct this diagram, we produced a catalog of objects in the optical images with the SExtractror software (Bertin and Arnouts 2016) from which the stars were excluded (CLASS_STAR > 0.8). The magnitudes of galaxies were determined within an adaptive aperture by Kron's method (Kron 1980, MAG_AUTO); the colors of galaxies were determined by comparing the magnitudes in identical apertures with a size equal to the FWHM of the PSF. The red sequence of cluster galaxies is seen in Fig. 3. It is a crowding of data points near the red horizontal line. The scatter of data points near this line roughly corresponds to the photometric measurement errors of the galaxy colors. Because of the large photometric measurement er-
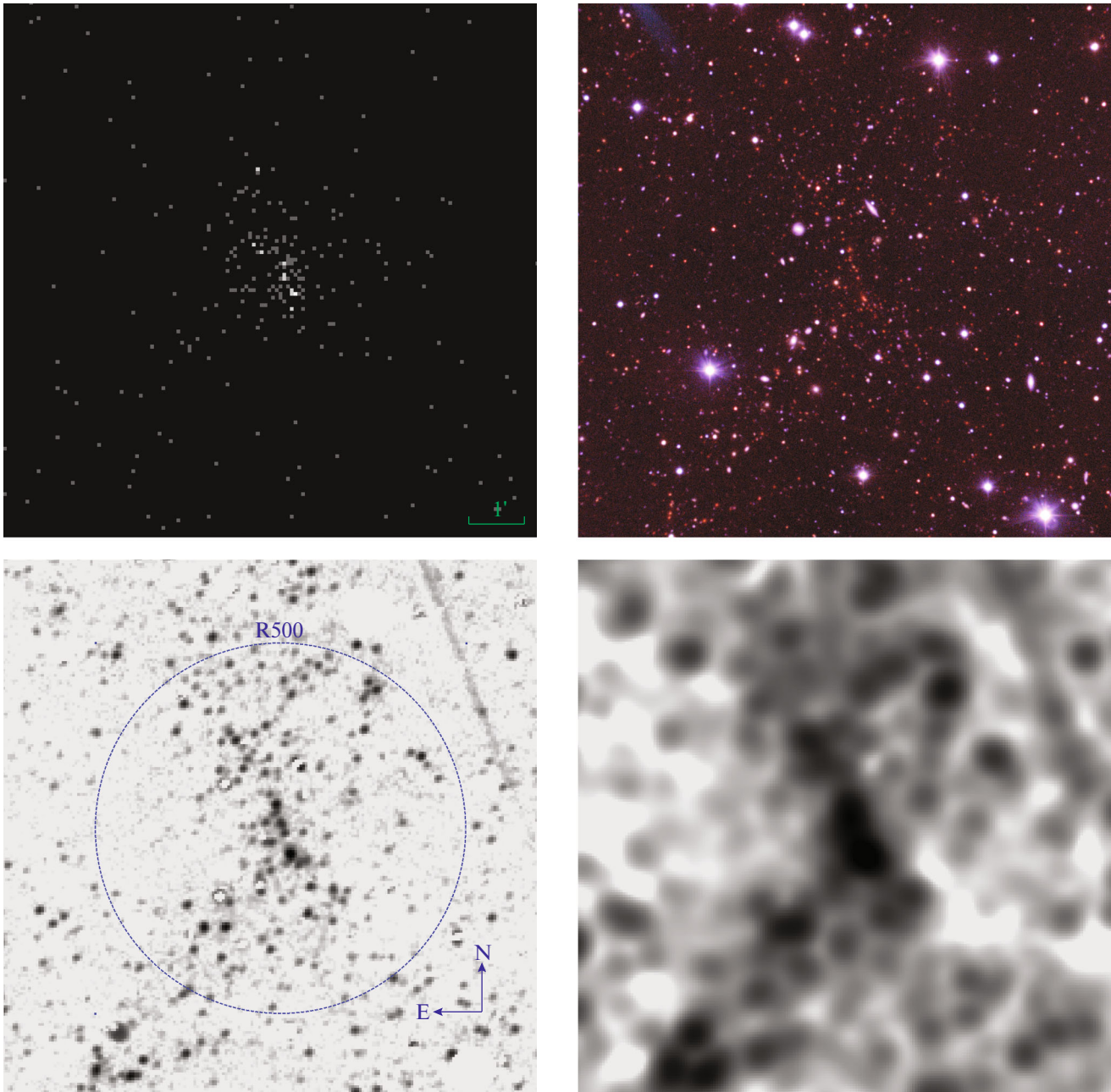
Fig. 2. An X-ray image of the field of the galaxy cluster SRGe CL2305.2−2248 from the SRG/eROSITA data (upper left panel), a pseudo-color image in the i, r, g (RGB) filters from the RTT-150 observations with a seeing $\sim 1\rlap{.}''5$ (upper right panel), a WISE image in the 3.4-μm band cleaned of stars and galaxies that do not belong to the cluster red sequence (lower left panel), and the same image smoothed by a two-dimensional Gaussian, $\sigma = 8''$ (lower right panel). A circle of radius $R_{500} = 3\rlap{.}'3$ is shown in the image on the lower right panel. All images are presented on the same scale, the field size is $9\rlap{.}'4 \times 9\rlap{.}'4$, the center of the field coincides with the X-ray center of the cluster.

rors, it is impossible to obtain a reliable measurement of the slope of the red sequence and the intrinsic scatter of colors.

The images from the WISE infrared all-sky survey are shown at the bottom in Fig. 2. The models of all the objects that do not belong to the cluster red sequence were subtracted from these images.

The image on the lower right panel was additionally smoothed by a two-dimensional Gaussian, $\sigma = 8''$. These images show the distribution of cluster galaxies in the plane of the sky. It can be seen that in the central region of the cluster ~ 1 arcmin in size the distribution of galaxies is elongated in the NNE−SSW direction. At the cluster redshift (see below) this size
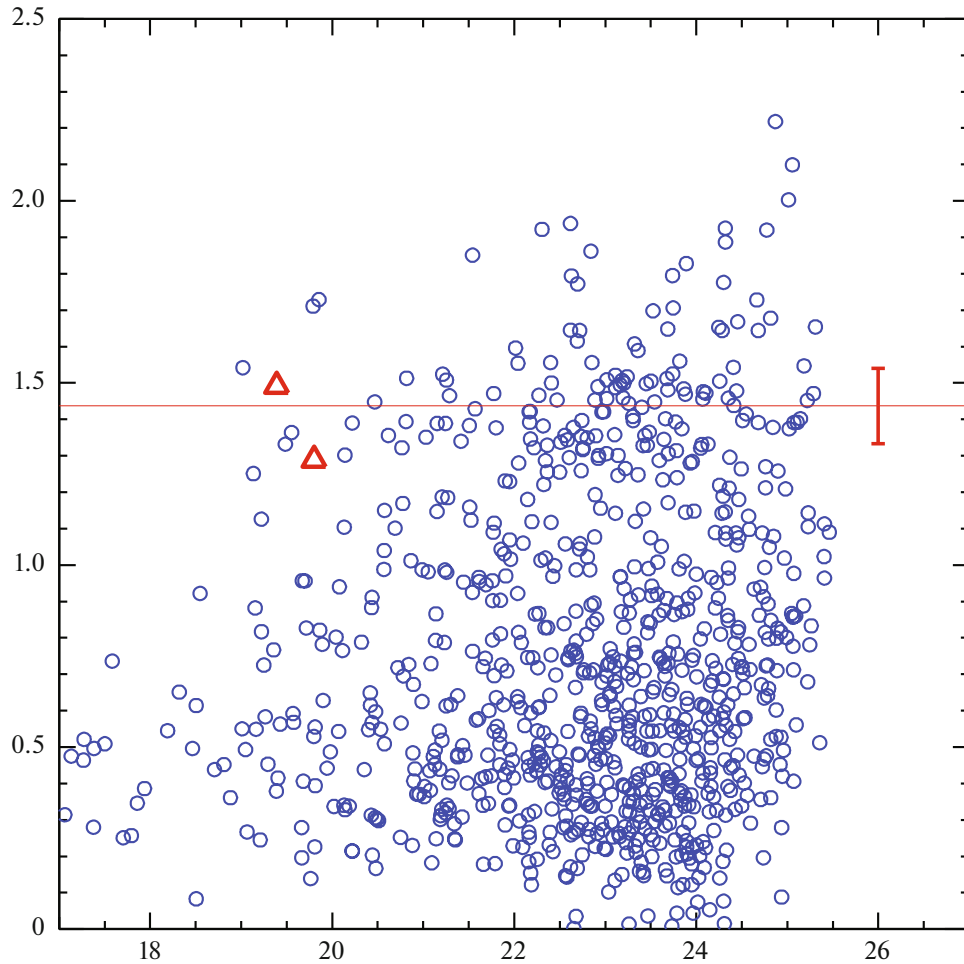
Fig. 3. Color−magnitude diagram for galaxies within 3.'3 of the center of the cluster SRGe CL2305.2−2248. The position of the red sequence of cluster galaxies is marked by the horizontal straight line, the vertical bar indicates the typical color measurement error for each individual galaxy. The red triangles indicate the central cluster galaxies for which the spectroscopic redshifts were measured.

corresponds to a size ∼500 kpc. At greater distances from the center the distribution of cluster galaxies in the plane of the sky also remains nonuniform. In the eastward and westward directions no cluster galaxies are observed already at a distance less than 1 arcmin from the cluster center, while in the northward and southward directions the surface density of cluster galaxies remains significant up to distances of the order of or greater than $R_{500} \approx 3'$ (see below). The shape of the distribution of galaxies in the plane of the sky resembles an hourglass. Such a strong central asymmetry of the distribution of galaxies in the plane of the sky may suggest that the cluster is not a relaxed one.

3.2. Photometric Redshift Estimate for the Cluster Using Machine Learning

As has been shown (see, e.g., Meshcheryakov et al. 2015), machine learning methods allow the photometric redshifts (photo-z) of galaxy clusters to be

measured with a high accuracy from individual galaxies (in particular, an accuracy $\sigma \sim 1\%$ was achieved for clusters at $z < 0.45$ using SDSS data (Meshcheryakov et al. 2015)). We trained the photo-z model for galaxies based on a quantile random forest described in Meshcheryakov et al. (2018) on a training sample one million galaxies in size from the SDSS DR16 spectroscopic survey. The magnitudes from the Pan-STARRS1 DR2 catalog obtained by fitting the PSF and the method of Kron (1980), the W1 and W2 magnitudes derived from WISE forced photometry in the corresponding filters (Burenin et al. 2021), and all possible colors based on these optical and infrared magnitudes acted as photometric attributes for the random forest model. Using this model of photometric z estimates, we made redshift predictions for all of the optical galaxies in the field of the cluster SRGe CL2305.2−2248. Next, we filtered out only the objects with reliable predictions in confidence parameter `zConf` > 0.6, with `zConf` having been defined
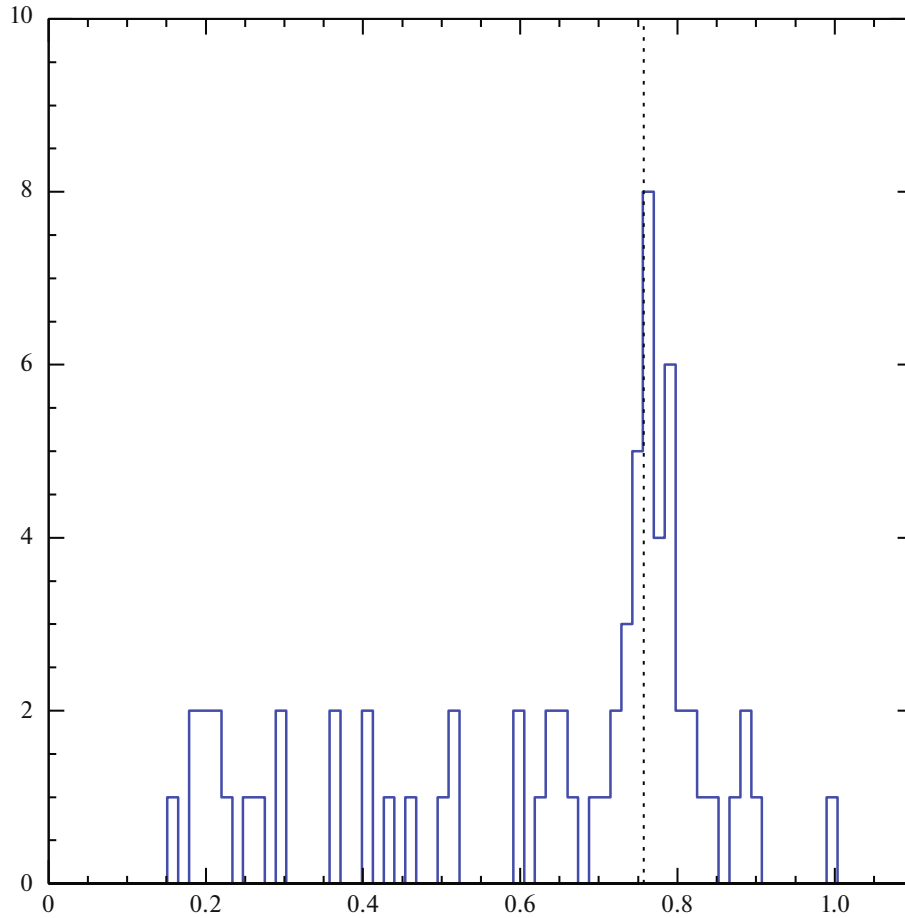
Fig. 4. Distribution of galaxies in the SRGe CL2305.2−2248 field located within 2′ of the X-ray center of the cluster in photometric redshift. The photometric redshift estimates were obtained from the Pan-STARRS and WISE data using machine learning methods. The spectroscopic redshift measurement, $z = 0.7573$, is indicated by the vertical dotted line.

in a standard way as the probability of the prediction of a photometric z estimate in the vicinity of $z_{phot} \pm 0.06(1 + z_{phot})$.

Figure 4 shows the distribution of galaxies located within 2′ of the X-ray center of the cluster in photometric redshift estimate. The distribution has a clearly distinguishable peak, from which a photometric redshift estimate for the cluster can be obtained: $z_{phot} = 0.766 \pm 0.012$.

3.3. Spectroscopy

The spectra of the brightest galaxies in distant clusters were taken at the 6-m SAO RAS telescope with the SCORPIO-2 instrument (Afanasiev and Moiseev 2011). The observations were carried out during the night of August 17, 2020. The position angle of the long slit was chosen so that two central galaxies with coordinates $\alpha = 23^h05^m10\overset{s}{.}6$, $\delta = -22^d49^m11^s$ and magnitudes $i = 19.39$ and 19.80 fell into the slit. The slit width was 1″.97 at seeing 1″.8.

The spectrum was taken with the VPHG940@600 grism in the spectral range 3500−8500 Å, the spectral resolution was about 14 Å. The total exposure time was 4800 s, it was divided into four 1200-s exposure times between which the objects were shifted along the slit by 14″.

The spectroscopic data were reduced in a standard way, using the IRAF[3] software package and our own software. The images of two-dimensional spectra were bias subtracted, flat fielded, and transformed to the wavelength scale based on the spectra of calibration lamps. Then, the two-dimensional spectra were aligned and added, the one-dimensional spectra of galaxies and the background spectra were extracted from the two-dimensional spectrum in a standard way. The flux density in the spectra was calibrated using the observations of spectrophotometric standards from the list of the European Southern Observatory.[4]

---

[3] http://iraf.noao.edu/.
[4] https://www.eso.org/sci/observing/tools/standards/.
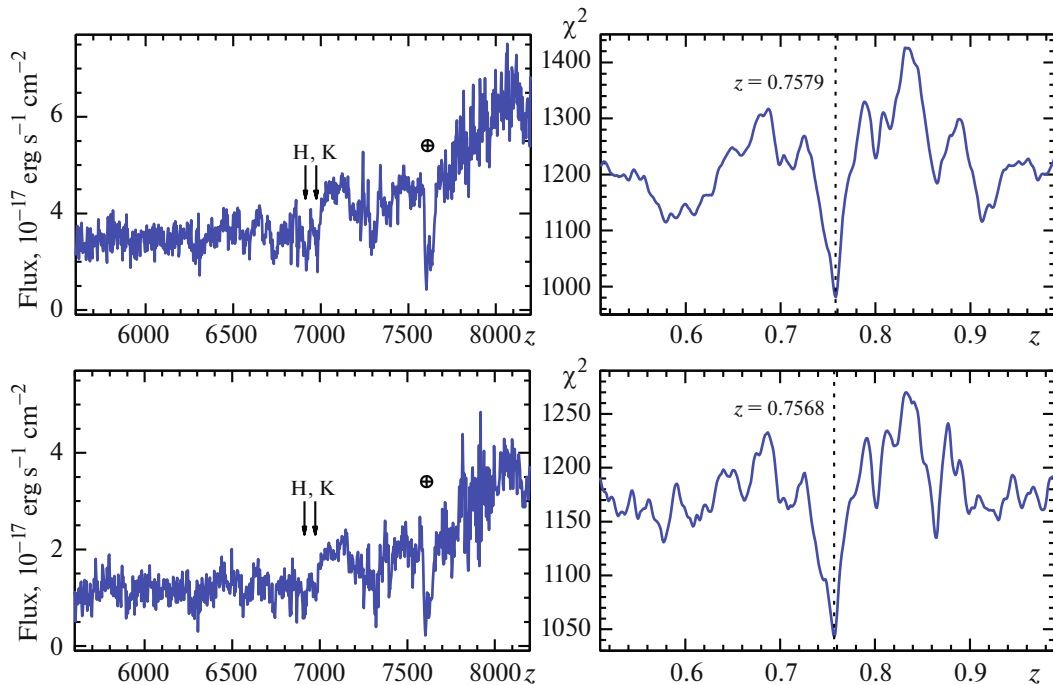
Fig. 5. Spectra of two central galaxies in the cluster SRGe CL2305.2−2248 taken at the 6-m SAO RAS BTA telescope with the SCORPIO-2 instrument (left). The redshift dependence of χ^2 from the cross-correlation of the spectra with the template of an elliptical galaxy (right).

The spectra of the two brightest cluster galaxies are shown in Fig. 5 on the left. Here, the absorption lines of the calcium H and K doublet and a break near 4000 Å are clearly seen. The redshift dependence of χ^2 from the cross-correlation of the spectra with the template of an elliptical galaxy is shown in Fig. 5 on the right. The measured redshifts of the two galaxies in the slit are close, $z_1 = 0.7579 \pm 0.0007$ and $z_2 = 0.7568 \pm 0.0009$, while the redshift determined from the sum of the spectra is $z = 0.7573 \pm 0.0006$. Since these galaxies belong to the red sequence of cluster galaxies and are close to the cluster center, this may be deemed to be the redshift measurement for the entire galaxy cluster with a high degree of reliability. The spectroscopic redshift measurement for the cluster obtained from the observations at the 6-m BTA telescope is in good agreement with the above photometric estimates.

4. MASS ESTIMATES FOR THE CLUSTER SRGe J2305.2−2248

At redshift $z = 0.7573$ the X-ray flux from the cluster measured above corresponds to an X-ray luminosity of $(1.20 \pm 0.11) \times 10^{45}$ erg s^{-1}. Using the calibration of the X-ray luminosity−mass relation from Vikhlinin et al. (2009a), we can estimate the cluster mass. A comparison of the masses of rich clusters at redshifts $z > 0.3$ derived using this relation from the X-ray luminosity measurements in the SRG/eROSITA survey with the masses measured through the observation of the SZ effect in the Planck survey taken from the PSZ2 catalog shows that the mass estimates from the X-ray data are, on average, higher by 12.8%. The mass of the cluster SRGe CL2305.2−2248 estimated from its X-ray luminosity and scaled to the masses measured in the Planck survey is $M_{500} = (9.03 \pm 2.56) \times 10^{14}\ M_\odot$, where the scatter of the mass−luminosity relation gives a major contribution to the error in the cluster mass estimate. According to the scaling relations from Vikhlinin et al. (2009a), a cluster of such a mass must have a temperature $T = 11.6 \pm 2.1$ keV. A galaxy cluster of such a mass is among only a few most massive clusters at redshifts $z > 0.6$ (for a discussion, see below).

Using the measurements of the parameters of galaxy clusters for a sample of relaxed clusters based on Chandra data (Vikhlinin et al. 2006), we can estimate the radius $R_{500} = 1430 \pm 120$ kpc for the cluster SRGe CL2305.2−2248, corresponding to an angular size of about $3'.3$.

The cluster SRGe CL2305.2−2248 was not detected in the Planck all-sky survey trough the observation of the SZ effect (Sunyaev and Zeldovich 1972) above a significance level high enough to be included

in the PSZ2 catalog. However, we detected the SZ source at a lower significance level in this field on the Planck all-sky survey Comptonization parameter maps that were prepared as was done in Burenin (2017). This cluster was detected previously in the Atacama Cosmology Telescope (ACT, Hilton et al. 2021) and South Pole Telescope (SPT, Bleem et al. 2020) surveys. According to the ACT data, the cluster mass scaled to the masses in the PSZ2 catalog is $M_{500} = (9.18 \pm 1.48) \times 10^{14}\ M_\odot$, while the same mass of this cluster from the SPT data is $M_{500} = (7.40 \pm 0.83) \times 10^{14}\ M_\odot$. In both cases, the catalogs of these surveys provide only the photometric redshift estimates for this cluster.

4.1. Joint Analysis of the Data in the X-ray and Microwave Bands

The importance of a joint analysis of the X-ray and microwave observations of the hot gas in galaxy clusters was discussed long before the confident detection of the SZ effect. For example, measurements of the X-ray flux from the hot intergalactic gas in a galaxy cluster (the radiation intensity is determined by the emission measure proportional to the gas density squared) and the reduction in the brightness of the cosmic microwave background toward the cluster due to the SZ effect (proportional to the gas density) make it possible to determine the distance to the cluster, i.e., its redshift (for a discussion, see Sunyaev and Zeldovich 1980).

In light of the appearance of large-scale and sensitive surveys in the X-ray (SRG/eROSITA) and microwave (Planck, SPT, and ACT) bands, the estimates of galaxy cluster parameters based only on the F_X and Y measurements are of special interest (see, e.g., Churazov et al. 2015). This approach does not replace the photometric or spectroscopic z measurements, but allows one to immediately make rough mass estimates for clusters (or cluster candidates) and to optimize the programs of optical observations by focusing on the most massive clusters. The specific optimization procedure will be published separately. For the cluster under consideration we know F_X, Y, and z. Therefore, it is interesting to check whether all approaches are compatible.

Given the X-ray flux F_X and the redshift z, we can use the luminosity−temperature and luminosity−mass relations to determine the cluster parameters.[5]

---

[5] If the X-ray data allow the temperature T_X and the mass of the gas M_g to be reliably measured, then we can also use such quantities as, for example, $Y_X \propto T_X \times M_g$ or directly M_g to estimate the total cluster mass (see, e.g., Kravtsov et al. 2006).

Similarly, we can use the total Comptonization parameter Y in combination with z.

First of all, for clusters at redshifts $z \sim 0.6-2$ the mass can be roughly estimated (to within a factor ~ 2) directly from the X-ray flux F_X (Eq. (13) from Churazov et al. (2015)): $M_{500} \approx 1.2 \times 10^{14} \left(\frac{F_X}{10^{-14}} \right)^{0.57} \approx 1.3 \times 10^{15}\ M_\odot$. This relation does not directly use the redshift, except for the assumption that $z \gtrsim 0.6$. The mass estimate obtained is indeed consistent, within a factor of 2, with the estimate based on the luminosity−mass relation for a known z (see above).

Another interesting possibility is to estimate z from the measured F_X and Y. In the simplest case, $R_{XSZ} = F_X/Y$ correlates well with z for moderately close ($z > 0.6$) clusters (Aghanim et al. 2012; Churazov et al. 2015). The combination of SRG/eROSITA data with the ACT catalogs (Hilton et al. 2021) seems particularly attractive because of the large overlap of the surveyed sky regions.

The parameters of the correlation of the redshift with the X-ray and microwave data depend on the specific method of measuring the intensity of radiation from clusters. In particular, the ACT catalogs provide $y_{c,\text{fixed}}$ specifying the normalization of the tSZ signal from the cluster for a fixed geometry of the spatial filter. The choice of a fixed filter actually means that the maps obtained by different telescopes after their convolution with specified filters can be compared directly. It turns out that, in this case, the relation between z and the ratio of the signals in the X-ray and microwave bands can be written, for example, as

$$\frac{F_{X,\text{fixed}}}{y_{c,\text{fixed}}} \approx 2.9 \times 10^{-9} z^{-0.85}\ \text{erg s}^{-1}\ \text{cm}^{-2}, \quad (1)$$

where $F_{X,\text{fixed}}$ is the flux in the 0.4−2 keV energy band for the fixed spatial filter used in the search for clusters in the X-ray band. The parameters of this relation were calibrated for a set of clusters detected in both X-ray and microwave bands by taking into account the specific flux measurement algorithm. Applying this relation to the cluster SRGe CL2305.2−2248 ($F_{X,\text{fixed}} \approx (1.25 \pm 0.15) \times 10^{-12}$ erg s^{-1} cm^{-2}; $y_{c,\text{fixed}} \approx 3.14 \times 10^{-4}$) gives a redshift estimate $z \approx 0.7 \pm 0.1$. Note that for the chosen fixed spatial filter the X-ray flux from the cluster SRGe CL2305.2−2248 is approximately twice as high as the directly measured flux discussed above. Despite the inevitable significant uncertainty in measuring z by this method, such estimates help to immediately classify this cluster as a potentially distant object.
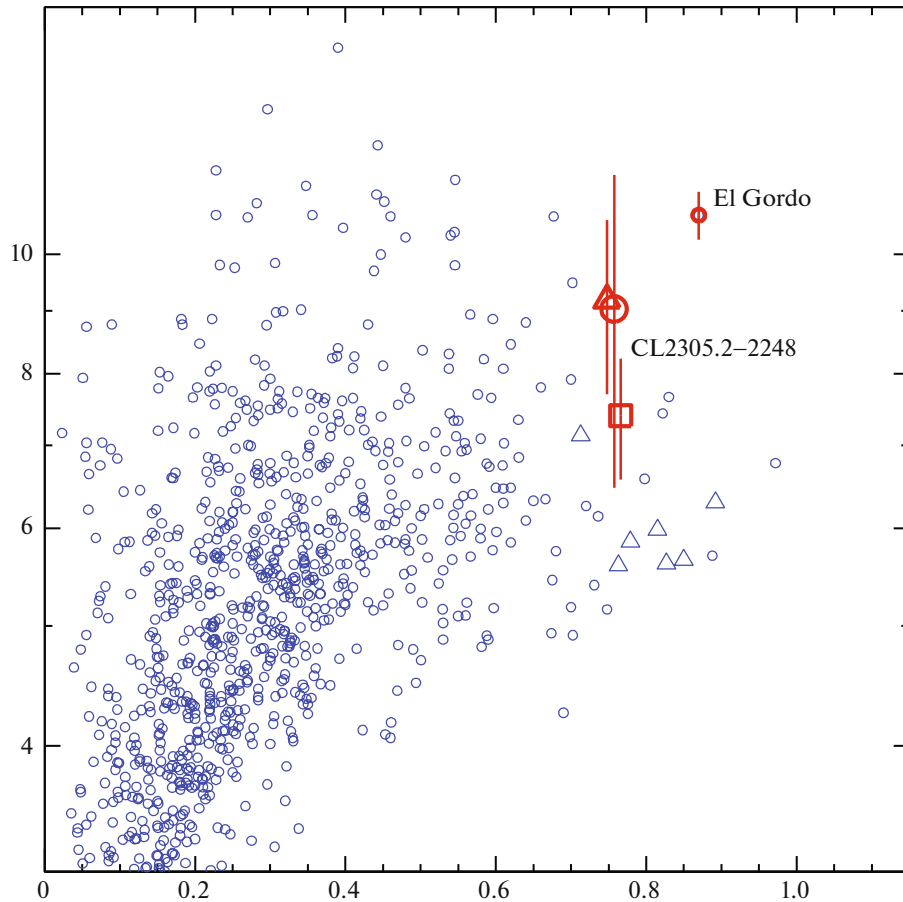
Fig. 6. Distribution of galaxy clusters in the redshift−mass M_{500} plane. The red symbols indicate the mass estimates for the cluster SRGe CL2305.2−2248 from the SRG/eROSITA (circle), ACT (triangle), and SPT (square) data. For comparison, the red circle also indicates the mass measurement for the very massive galaxy cluster El Gordo (Menanteau et al. 2012) taken from the second Planck catalog. The blue circles indicate the galaxy clusters from the PSZ2 catalog, the blue triangles indicate the clusters from the PSZ2 catalog identified in the work of our group (Burenin et al. 2018).

5. DISCUSSION

Massive galaxy clusters, with masses of the order of $M_{500} \approx 10^{15} \ M_{\odot}$, are extremely rare objects. Based on our observations at the 6-m BTA telescope, we measured the spectroscopic redshift for the cluster SRGe CL2305.2−2248, $z = 0.7573$, which is in good agreement with the photometric redshift estimates. Based on the SRG/eROSITA X-ray data, we estimated the cluster mass to be $M_{500} = (9.03 \pm 2.56) \times 10^{14} \ M_{\odot}$. According to the mass−temperature scaling relation, a cluster with such a mass must have a temperature $T = 11.6 \pm 2.1$ keV. The high cluster mass is also confirmed by the ACT data, which give a measurement of $M_{500} = (9.18 \pm 1.48) \times 10^{14} \ M_{\odot}$, and the SPT data, $M_{500} = (7.40 \pm 0.83) \times 10^{14} \ M_{\odot}$. All these estimates of the cluster mass were scaled to the masses of clusters in the second Planck SZ source catalog (PSZ2).

A galaxy cluster with such a mass must be among only several tens of the most massive clusters in the observable Universe and among only a few most massive clusters ar redshifts $z > 0.6$. This is shown in Fig. 6. The well-known very massive galaxy cluster El Gordo (Menanteau et al. 2012) is also marked in the same figure. The mass of the cluster SRGe CL2305.2−2248 turns out to be comparable to the mass of the cluster El Gordo.

In the X-ray band the central part of the cluster looks perturbed, which may be the result of an outflow of hot gas from the active nucleus of one of the central galaxies in the cluster. On the other hand, this may be a consequence of large-scale gas motions, which can arise, for example, due to a recent merger with a less massive cluster.

The distribution of galaxies in the plane of the sky has a shape resembling an hourglass—in the eastward and westward directions no cluster galaxies are observed already at a distance less than 1 arcmin from the cluster center, while in the northward and southward directions the surface density of cluster galaxies remains significant up to distances of the

order of or greater than $R_{500} \approx 3\overset{\prime}{.}3$. Such a strong central asymmetry of the distribution of galaxies in the plane of the sky may suggest that the dynamical state of the cluster is an unsteady one.

Galaxy clusters of such a large mass are unique objects in the observable Universe and deserve a further detailed study.

REFERENCES

1. P. A. R. Ade, N. Aghanim, C. Armitage-Caplan, M. Arnaud, M. Ashdown, et al. (Planck Collab.), Astron. Astrophys. **571**, A20 (2014).
2. P. A. R. Ade, N. Aghanim, M. Arnaud, M. Ashdown, J. Aumont, et al. (Planck Collab.), Astron. Astrophys. **594**, A27 (2016a).
3. P. A. R. Ade, N. Aghanim, M. Arnaud, M. Ashdown, J. Aumont, et al. (Planck Collab.), Astron. Astrophys. **594**, A24 (2016b).
4. V. L. Afanasiev and A. V. Moiseev, Baltic Astron. **20**, 363 (2011).
5. N. Aghanim, M. Arnaud, M. Ashdown, F. Atrio-Barandela, J. Aumont, et al. (Planck Collab.), Astron. Astrophys. **543**, A102 (2012).
6. E. Bertin and S. Arnouts, Astron. Astrophys. Suppl. Ser. **117**, 393 (1996).
7. L. E. Bleem, S. Bocquet, B. Stalder, M. D. Gladders, P. A. R. Ade, S. W. Allen, et al., astrophys. J. Suppl. Ser. **247**, 25 (2020).
8. R. A. Burenin, Astron. Lett. **43**, 507 (2017).
9. R. A. Burenin, I. F. Bikmaev, I. M. Khamitov, I. A. Zaznobin, G. A. Khorunzhev, M. V. Eselevich, V. L. Afanas'ev, S. N. Dodonov, J. A. Rubino-Martin, N. Aghanim, and R. A. Syunyaev, Astron. Lett. **44**, 297 (2018).
10. R. A. Burenin et al., (2021, in preparation).
11. A. Cavaliere and R. Fusco-Femiano, Astron. Astrophys. **500**, 95 (1976).
12. K. C. Chambers, E. A. Magnier, N. Metcalfe, H. A. Flewelling, M. E. Huber, C. Z. Waters, et al., arXiv:1612.05560 (2016).
13. E. Churazov, A. Vikhlinin, and R. Sunyaev, Mon. Not. R. Astron. Soc. **450**, 1984 (2015).
14. M. Hilton, C. Sifon, S. Naess, M. Madhavacheril, M. Oguri, E. Rozo, et al., Astrophys. J. Suppl. Ser. **253**, 3 (2021).
15. B. l'Huillier, A. Shafieloo, D. Polarski, and A. A. Starobinsky, Mon. Not. R. Astron. Soc. **494**, 819 (2020).
16. A. V. Kravtsov, A. Vikhlinin, and D. Nagai, Astrophys. J. **650**, 128 (2006).
17. R. G. Kron, Astrophys. J. Suppl. Ser. **43**, 305 (1980).
18. A. M. Meisner, D. Lang, and D. J. Schlegel, Astron. J. **154**, 161 (2017).
19. F. Menanteau, J. P. Hughes, C. Sifon, M. Hilton, J. Gonzalez, L. Infante, et al., Astrophys. J. **748**, 7 (2012).
20. A. V. Meshcheryakov, V. V. Glazkova, S. V. Gerasimov, R. A. Burenin, and G. A. Khorunzhev, Astron. Lett. **41**, 307 (2015).
21. A. V. Meshcheryakov, V. V. Glazkova, S. V. Gerasimov, and I. V. Mashechkin, Astron. Lett. **44**, 735 (2018).
22. P. Predehl, R. Andritschke, V. Arefiev, V. Babyshkin, O. Batanov, W. Becker, et al., Astron. Astrophys. **647**, A1 (2021).

23. R. A. Sunyaev and Y. B. Zeldovich, Comm. Astrophys. Space Phys. **4**, 173 (1972).
24. R. A. Sunyaev and Y. B. Zeldovich, Ann. Rev. Astron. Astrophys. **18**, 537 (1980).
25. R. A. Sunyaev, V. Arefiev, V. Babyshkin, A. Bogomolov, K. Borisov, M. Buntov, et al., arXiv:2104.13267 (2021).
26. A. Vikhlinin, B. R. McNamara, W. Forman, C. Jones, H. Quintana, and A. Hornstrup, Astrophys. J. **502**, 558 (1998).
27. A. Vikhlinin, A. Kravtsov, W. Forman, C. Jones, M. Markevitch, S. S. Murray, et al., Astrophys. J. **640**, 691 (2006).
28. A. Vikhlinin, R. A. Burenin, H. Ebeling, W. R. Forman, A. Hornstrup, C. Jones, et al., Astrophys. J. **692**, 1033 (2009a).

29. A. Vikhlinin, A. V. Kravtsov, R. A. Burenin, H. Ebeling, W. R. Forman, A. Hornstrup, et al., Astrophys. J. **692**, 1060 (2009b).
30. E. L. Wright, P. R. M. Eisenhardt, A. K. Mainzer, M. E. Ressler, R. M. Cutri, T. Jarrett, et al., Astron. J. **140**, 1868 (2010).
31. I. A. Zaznobin, R. A. Burenin, I. F. Bikmaev, I. M. Khamitov, G. A. Khorunzhev, G. A. Konoplev, M. V. Eselevich, V. L. Afanas'ev, S. N. Dodonov, J.-A. Rubino-Martin, N. Aghanim, and R. A. Syunyaev, Astron. Lett. **45**, 49 (2019).

Translated by V. Astakhov